www.ietdl.org

Published in IET Microwaves, Antennas & Propagation
Received on 25th September 2013
Revised on 5th August 2014
Accepted on 29th August 2014
doi: 10.1049/iet-map.2013.0528

ISSN 1751-8725

Non-linearity in superconducting coplanar waveguide rectangular-spiral resonators

S. Mohammad Hassan Javadzadeh[1], *Alessandro Bruno*[2], *Forouhar Farzaneh*[3], *Mehdi Fardmanesh*[3]

[1]*Department of Electrical Engineering, Shahed University, Tehran, P.O. Box 18155/159, Iran*
[2]*Faculty of Applied Sciences, Kavli Institute of NanoScience, Delft University of Technology, Lorentzweg 1, 2628 CJ Delft, The Netherlands*
[3]*School of Electrical Engineering, Sharif University of Technology, Tehran, Iran*
E-mail: smh.javadzadeh@shahed.ac.ir

Abstract: In the present work, a non-linear distributed circuit model for superconducting rectangular-spiral resonators is proposed. This is based on an accurate non-linear circuit model for superconducting parallel coupled lines, which is simultaneously considered both quadratic and modulus non-linear dependencies. The non-linearity in superconducting devices depends on the current distribution, which is mainly determined by the geometrical structure of the device. The current distribution in the superconducting spiral resonators can be computed by a numerical approach based on three-dimensional finite element method. This computed current distribution is used to produce a non-linear circuit model for the superconducting spiral resonator. Numerical technique based on harmonic balance approach is used for non-linear analysis of the proposed equivalent non-linear circuit. The model is proposed for coplanar waveguide (CPW) resonators, which can easily be extended for microstrip resonators. To confirm the accuracy of the proposed model, non-linearity in a 6-pole superconducting CPW spiral bandpass filter has been measured. Measurement results show good agreement with the ones from the model. This proposed technique is found to be a major approach for fast and efficient non-linear analysis of the superconducting spiral resonators and filters.

1 Introduction

The non-linear behaviour of the superconducting microwave components, caused by the dependence of the superfluid density of the superconductors on the current distribution [1–3], limits the power handling capability of these devices which leads to restriction of the many applications of the superconductors in the microwave modules. For example, the intermodulation distortion (IMD) is a serious limitation for the use of the superconducting components of the communication systems, especially for the use of the superconducting microwave filters [4, 5]. These limitations might be eased if engineers could reliably predict the non-linear effects in their designs.

Numerous measurement of non-linear effects such as IMD and harmonic generation are reported [6–8]. In addition, a number of non-linear models of superconducting microstrip transmission lines (MTLs) [9–11], superconducting bends [12, 13], superconducting parallel coupled lines [14] and superconducting discontinuities [15] have been reported in the literature. In [16], a non-linear circuit model for folded superconducting resonators, like hairpin lines and meander lines, which contain multiple symmetric coupled superconducting transmission lines, is developed. For spiral transmission lines there are no non-linear model yet available and mainly the full numerical methods are used. Therefore finding simple yet accurate enough non-linear circuit model for these superconducting structures is still welcomed in order to give up the seemingly unavoidable use of time- and memory-consuming numerical approaches for non-linear analysis.

Moreover, superconducting microwave filters have been used frequently for different goals [17]. Very low insertion loss, good sharpness and small size are the properties of superconducting filters which motivate scientists to use this kind of microwave filters. One of the novel types of compact planar microwave filters is the spiral filter, which uses single spiral resonators and can be realised in the forms of microstrip structure, made by superconductors [18], or normal conductors [19] as well as coplanar waveguides (CPWs) [20, 21]. Spiral resonators are not only very compact, but also have remarkable properties such as high Q-factor, high power capability and insensitivity to the fabrication process. Spiral resonators have been recently used for realising meta-surfaces and meta-materials [22, 23].

In this paper, a non-linear circuit model for superconducting CPW spiral resonators is proposed. First a non-linear circuit model is presented for CPW rectangular-spiral resonators. This circuit model is inferred from non-linear circuit model of superconducting coupled lines and superconducting discontinuities where all are based on accurate non-linear circuit model for transmission lines in [11], which simultaneously considers both kinds of non-linear dependency: modulus and quadratic. Then harmonic balance (HB) method using ADS software [24], has been employed to evaluate the non-linear performance of the structure.

To confirm the accuracy of the proposed model, a 6-pole superconducting CPW spiral filter has been fabricated and measured. This quasi-elliptic bandpass filter (BPF) has 400 MHz bandwidth around 6 GHz. Non-linear measurement is performed at 4.2 K and their results are compared with those obtained from the proposed non-linear model. This model is very useful for optimising the spiral resonators in the superconducting microwave structures in order to minimise their non-linear distortions and engineer the non-linearity. Although the proposed model is dedicated for CPW resonators, it can be easily extended for superconducting spiral resonators in the form of either microstrip or stripline by using a similar procedure.

The organisation of this paper is as follows. Section 2 presents the non-linear circuit model for a CPW superconducting rectangular-spiral resonator. Section 3 is dedicated to the fabrication of the superconducting CPW spiral filter and measurements in the linear regime of this filter is reported. In Section 4, the non-linearity in superconducting CPW spiral filter is measured and its results are compared with the results obtained from our proposed model. Finally, conclusions are drawn in Section 5.

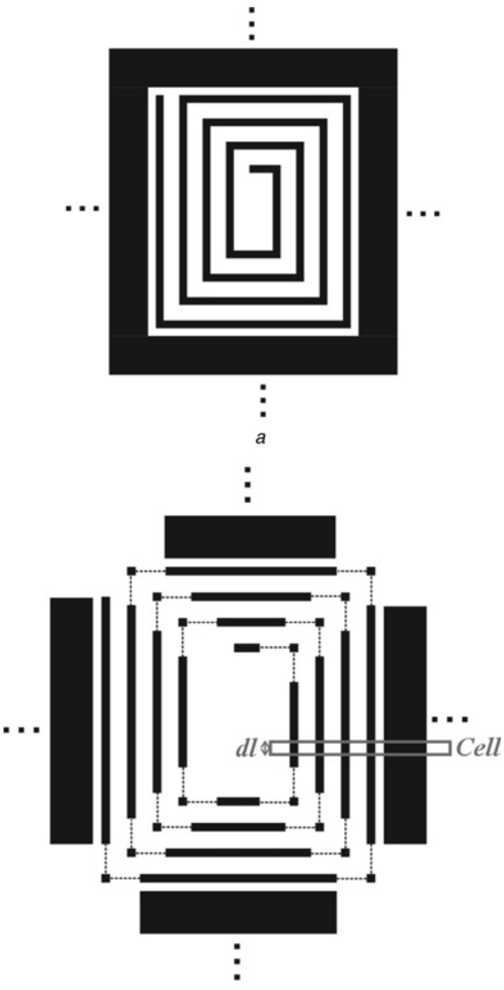

Fig. 1 *Non-linear circuit model*

a CPW spiral resonator
This figure shows a half-wavelength spiral resonator; in order to have a quarter-wavelength resonator we can easily connect the out end to ground for having a short circuit
b Equivalent structure for this spiral resonator, with the unit cell *dl*

2 Non-linear model

To propose a non-linear circuit model we consider rectangular-spiral resonator with N turns. A typical CPW spiral resonator with $N = 4$ is shown in Fig. 1*a*, where the ground plane is supposed to be large enough. This figure shows a half-wavelength spiral resonator, while a quarter wavelength resonator would have the outside end of the spiral resonator connected to the ground in order to have a short circuit. To work out a circuit model for this spiral structure, an equivalent structure can be considered, which is displayed in Fig. 1*b*.

Therefore each rectangular-spiral resonators with N turns consists of four coupled lines sections (CLSs), '$4N - 1$' straight bends and two open-ends (for half-wavelength resonators) or one open-end and one short circuit (for quarter-wavelength resonators). Each CLS consists of N coupled lines with different lengths and a half-plane of ground. Now we can divide each CLS to very small cells, as shown in Fig. 1*b*, and propose a non-linear distributed circuit model for each cell. A cell may consist of at least 1 and at most N coupled lines and also a half-plane of ground. Fig. 2 displays equivalent non-linear circuit for a cell with four lines. Although in this case $N = 4$, it can be easily extended for any value of N.

This circuit model of a cell in each CLS is deduced form non-linear circuit model of superconducting coupled lines

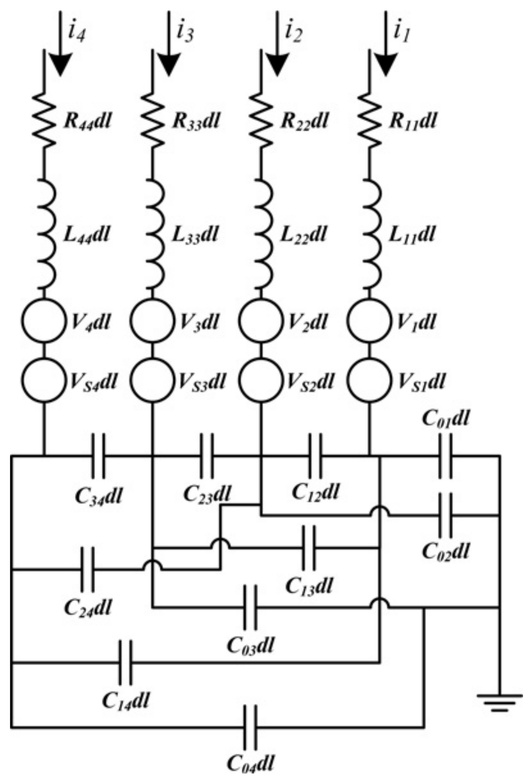

Fig. 2 *Equivalent non-linear circuit for a cell with N = 4 coupled lines*

Mutual resistance and inductance between the parallel lines are taken into account by equivalent voltage sources and non-linear contribution of all resistances and inductances are embedded in equivalent non-linear voltage sources
Although in this case $N = 4$, it can be easily extended for any value of N

in [16] based on the accurate non-linear circuit model for transmission lines in [11]. The mutual resistance and inductance between the parallel coupled lines are taken into account by equivalent voltage sources. For a voltage source in line m, in an equivalent circuit model of a cell with N coupled lines, we have

$$V_m = \sum_{\substack{n=1 \\ n\neq m}}^{N} \left(R_{mn} i_n + \frac{\mathrm{d}(L_{mn} i_n)}{\mathrm{d}t} \right) \tag{1}$$

where $m = 1, 2, \ldots, N$. These linear distributed parameters can be derived from RLGC matrices of multiconductor coupled lines [25, 26]. In addition, the non-linear parts of all resistances and inductances are taken into account by equivalent non-linear voltage sources. Considering a non-linear voltage source in line m, for the equivalent circuit model of a cell with N coupled lines, we have

$$V_{Sm} = \sum_{n=1}^{N} \left(\Delta R_{mn}(i_n, T) i_n + \frac{d\left(\Delta L_{mn}(i_n, T) i_n\right)}{dt} \right) \tag{2}$$

where T denotes temperature in Kelvin. Based on the proposed formulation in [11], we consider simultaneously both quadratic and modulus non-linear dependencies, for elements in the line m because of the current of line n, thus having

$$\Delta L_{mn}(i_n, T) = \Delta L^a_{mn}(T)\cdot i_n^2 + \Delta L^b_{mn}(T)\left|i_n\right|^3 + \Delta L^c_{mn}(T)\cdot i_n^4 + \Delta L^d_{mn}(T)\left|i_n\right|^5 + \Delta L^e_{mn}(T)\cdot i_n^6 \tag{3}$$

and for the resistance terms we have

$$\Delta R_{mn}(i_n, T) = \Delta R^a_{mn}(T)\cdot i_n^2 + \Delta R^b_{mn}(T)\left|i_n\right|^3 + \Delta R^c_{mn}(T)\cdot i_n^4 + \Delta R^d_{mn}(T)\left|i_n\right|^5 + \Delta R^e_{mn}(T)\cdot i_n^6 \tag{4}$$

where similar to the superconducting transmission lines [11], we have

$$\begin{aligned} \Delta L^a_{mn}(T) &= \Delta L^q_{mn}(T) \\ \Delta L^b_{mn}(T) &= 0.5\Delta L^{\mathrm{mod}}_{mn}(T)\alpha(T) \\ \Delta L^c_{mn}(T) &= -0.5\Delta L^q_{mn}(T)\alpha(T) \\ \Delta L^d_{mn}(T) &= 0.125\Delta L^{\mathrm{mod}}_{mn}(T)\alpha^2(T) \\ \Delta L^e_{mn}(T) &= -0.125\Delta L^q_{mn}(T)\alpha^2(T) \end{aligned} \tag{5}$$

and

$$\begin{aligned} \Delta R^a_{mn}(T) &= \Delta R^q_{mn}(T) \\ \Delta R^b_{mn}(T) &= 0.5\Delta R^{\mathrm{mod}}_{mn}(T)\alpha(T) \\ \Delta R^c_{mn}(T) &= -0.5\Delta R^q_{mn}(T)\alpha(T) \\ \Delta R^d_{mn}(T) &= 0.125\Delta R^{\mathrm{mod}}_{mn}(T)\alpha^2(T) \\ \Delta R^e_{mn}(T) &= -0.125\Delta R^q_{mn}(T)\alpha^2(T) \end{aligned} \tag{6}$$

The term $\alpha(T)$ can be calculated by the following equation [11]

$$\alpha(T) = \left(\frac{4T_C}{3\pi W t j_C T} \right)^2 \tag{7}$$

where T_C denotes critical temperature in Kelvin, j_C is the critical current of the superconducting thin film, W is the line width and t is the thickness of the superconducting layer.

If λ_L and σ_1, respectively, denote penetration depth and real part of conductivity in the superconductor, for quadratic non-linear terms we have

$$\Delta L^q_{mn}(T) = \frac{\mu_0 \lambda_L^2(T, 0)}{j_q^2(T)} \Lambda^q_{mn}(T) \tag{8}$$

and

$$\Delta R^q_{mn}(T) = \sigma_1(T, 0)\omega^2 \mu_0^2 \lambda_L^4(T, 0) \frac{2 + a(T)}{j_q^2(T)} \Lambda^q_{mn}(T) \tag{9}$$

where j_q is the non-linear scaling critical current for quadratic mode and $\Lambda^q_{mn}(T)$ is the quadratic geometrical non-linear factor. Then we have

$$\Lambda^q_{mn}(T) = \frac{\int j_m^2 j_n^2 \mathrm{d}S_m}{\left(\int j_m \mathrm{d}S_m\right)^2 \left(\int j_n \mathrm{d}S_n\right)^2} \tag{10}$$

where j_m and S_m, respectively, denote the volume current density and cross-section area of line m. For modulus non-linear terms we have

$$\Delta L^{\mathrm{mod}}_{mn}(T) = \frac{\mu_0 \lambda_L^2(T, 0)}{j_m(T)} \Lambda^{\mathrm{mod}}_{mn}(T) \tag{11}$$

and

$$\Delta R^{\mathrm{mod}}_{mn}(T) = \sigma_1(T, 0)\omega^2 \mu_0^2 \lambda_L^4(T, 0) \frac{2 + a(T)}{j_m(T)} \Lambda^{\mathrm{mod}}_{mn}(T) \tag{12}$$

where j_m is the non-linear scaling critical current for modulus mode and $\Lambda^{\mathrm{mod}}_{mn}(T)$ is the modulus geometrical non-linear factor and can be obtained by

$$\Lambda^{\mathrm{mod}}_{mn}(T) = \frac{\int j_m j_n^2 \mathrm{d}S_m}{\left(\int j_m \mathrm{d}S_m\right) \left(\int j_n \mathrm{d}S_n\right)^2} \tag{13}$$

In addition for each bend we can use a non-linear circuit model like in [27] and for open end a procedure similar to [28]. Therefore we just need to know current distribution in each line, which can be computed by solving the coupled Maxwell's and London's equations using numerical methods like three-dimensional finite element method (3D-FEM) with traditional software's like COMSOL [29] as explained in [15].

3 6-Pole spiral filter

To validate the accuracy of the proposed non-linear circuit model, a superconducting CPW spiral filter has been made and measured. The considered filter is a 6-pole BPF with bandwidth of 400 MHz about 6 GHz made of 300 nm thick NbTiN on 525 μm thick silicon substrate which has been

doi: 10.1049/iet-map.2013.0528

reported in [30]. We selected CPW quarter wavelength resonators which in addition to more compact sizes if compared to half-wavelength ones, have the capability of a farther second passband and do not have a passband at twice the centre frequency. Non-adjacent coupling causes the filter to show quasi-elliptic frequency response (two transmission zeros in both sides of the passband).

CPW microwave filters are the best choices for realising microwave integrated circuits (MICs) and on-chip microwave signal conditioning. A common drawback of CPW filters is the excitation of slot-line mode. The best solution for suppressing slot-line mode is to electrically connect the two grounds on both sides of the centre line of the CPW in order to equalise their potential. For this purpose, wire bonding can be employed, but more accurate and reproducible method is through the implementation of lithographed air bridges. Moreover, compared with microstrip structure, CPW is more suitable for quarter-wavelength-resonator filters. This is because grounding of CPW circuits requires no vias because of having the ground planes on the same substrate surface as the signal line. Using single-side deposited film on the substrate also simplifies the fabrication process.

For simulation of designed filter we used Sonnet EM software [31]. Each designed resonator has an area of 0.74 mm × 0.57 mm with a line width and gap of 30 μm between the adjacent lines. Fig. 3 shows the general configuration of the designed quasi-elliptic BPF. The input and output transmission line is a 50 Ω CPW transmission line with the linewidth of 30 μm and the gap of 20 μm.

An important note in the design of superconducting filters is that kinetic inductance has to be estimated and considered in the simulations. From the measured critical temperature and normal state resistivity of the 300 nm thick NbTiN films, we calculated $Ls = 0.8$ pH/sq and we used this value in the definition of the superconductor in Sonnet. The resulting filter geometry lead to a spectral response perfectly centred at 6 GHz, as desired.

We realised test samples of the filters on 20 mm × 4 mm silicon substrate having a thickness of 525 μm. The superconducting layer is sputter-deposited in a 3 mTorr

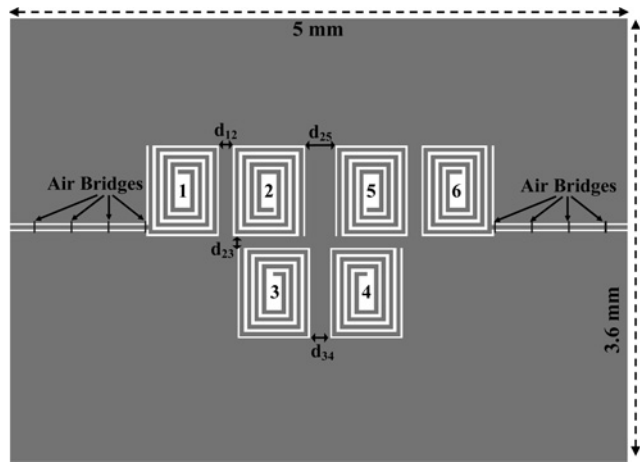

Fig. 3 *Configuration of the designed quasi-elliptic 6-pole BPF*

Non-adjacent coupling between the two resonators 2 and 5 causes two transmission zeros in the filter frequency response
Area considered for the simulation in Sonnet is 5 mm × 3.6 mm
We have $d_{12} = 110$ μm, $d_{23} = 70$ μm, $d_{34} = 160$ μm and $d_{25} = 240$ μm
Air bridges are shown in the figure, and their position and their number must be considered in the simulations

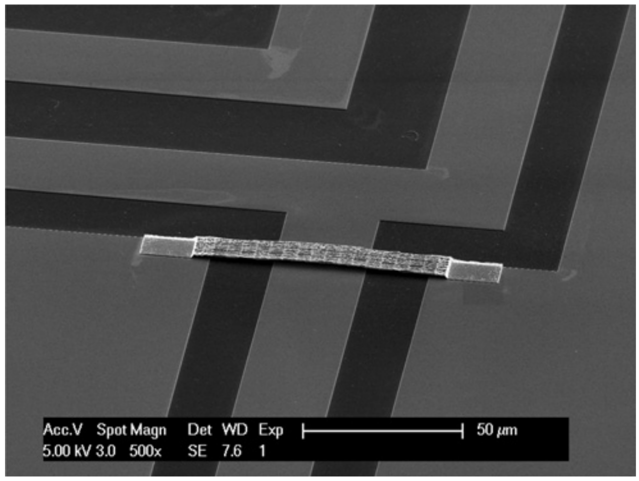

Fig. 4 *SEM picture of the realised air-bridge for the 6-pole BPF*

Each air bridge has the length of 75 μm and width of 10 μm and is made of a titanium/aluminium bilayer

Ar/N_2 atmosphere [32, 33]. For patterning the structure, EBPG (electron beam pattern generator, which is known as the electron beam lithography) is used in combination with polymethyl methacrylate (PMMA) resist. Reactive ion etching was employed in order to etch the patterned structure. The realisation of the air bridges required a single PMMA layer, exposed at variable doses: full dose (of about 1300 μC/cm^2) for the ground contacts, and a gradient of lower doses for the bridged sections. Careful choice of the development time allowed the resulting PMMA structure to be capable of lifting off a subsequent evaporation of a Ti/Al bilayer. The titanium layer was necessary in order to improve the adhesion.

Fig. 4 shows SEM (scanning electron microscope) picture of one of the fabricated air bridges. Each air bridge has the length of 75 μm, a width of 10 μm and approximately height of 2 μm in its middle.

Fig. 5 shows the measured results of the 6-pole quasi-elliptic filter in comparison with the simulation results from SONNET EM. Measured results have good agreement with simulation results. Insertion loss of the filter is very

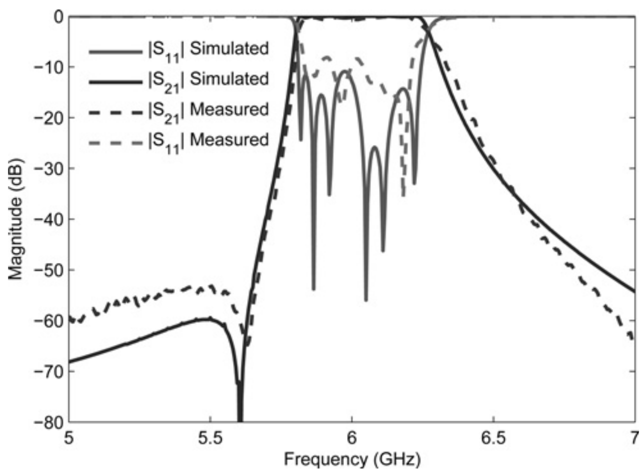

Fig. 5 *Comparison simulation and measurement results of the scattering parameters of the 6-pole BPF*

Owing to using superconducting material, insertion loss in the passband of filter is very small

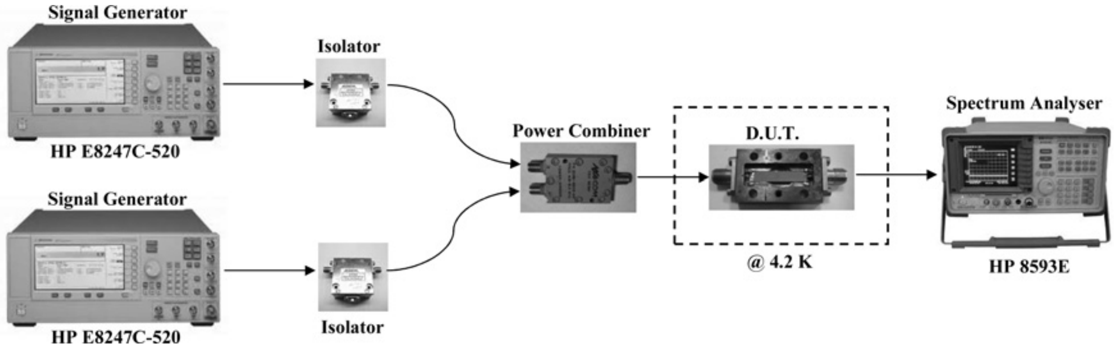

Fig. 6 *Our measurement set-up which it is used for non-linear measurement of superconducting microwave filter*
D.U.T. (the device under test)

small, which comes from the inherent property of superconductor resonators.

4 Measurements and discussions

For modelling the 6-pole spiral filter we used the proposed model for superconducting CPW spiral resonators and extended it to cover the coupling between the adjacent spiral resonators. To take into account this coupling effect, we define new cells for each two parallel coupled CLSs (from two separate spiral resonators). These new cells are equal to the combination of two normal cells and consist of at least two and at most $2N$ parallel coupled lines. Hence we have an equivalent non-linear circuit for our 6-pole CPW spiral filter. It is noticeable that for using the proposed non-linear model we should consider fitting parameters, which we consider critical current (J_C) as fitting parameter. All other modelling parameters can be measured. T_C was 15.5 K, magnetic penetration depth (λ_L) was 285 nm and the real part of conductivity (σ_1) was 68.96 S/m (resistivity was 145 µcm). Thereafter, with HB analysis of the obtained equivalent circuit, the convenient quantitative measure of non-linearity like third-order IMD can be calculated. In considering the air bridges in the equivalent circuit, we can use the linear circuit model from [34], although we neglect their non-linear effects.

For measurement of IMD in the fabricated spiral filter, we used a conventional set-up for non-linear measurements which used two similar oscillators, two isolators, a power combiner and a spectrum analyser as shown in Fig. 6. The filter box is sinked in liquid helium to cool at a temperature of 4.2 K.

We measured third-order IMD at different powers and frequencies in the range of passband frequencies of the filter at 4.2 K. Input-power dependence of the amplitude of the fundamental signal and the calculated and measured third-order upper sideband IMD signals in the mentioned BPF at two different frequencies of 5.9 and 6 GHz, for

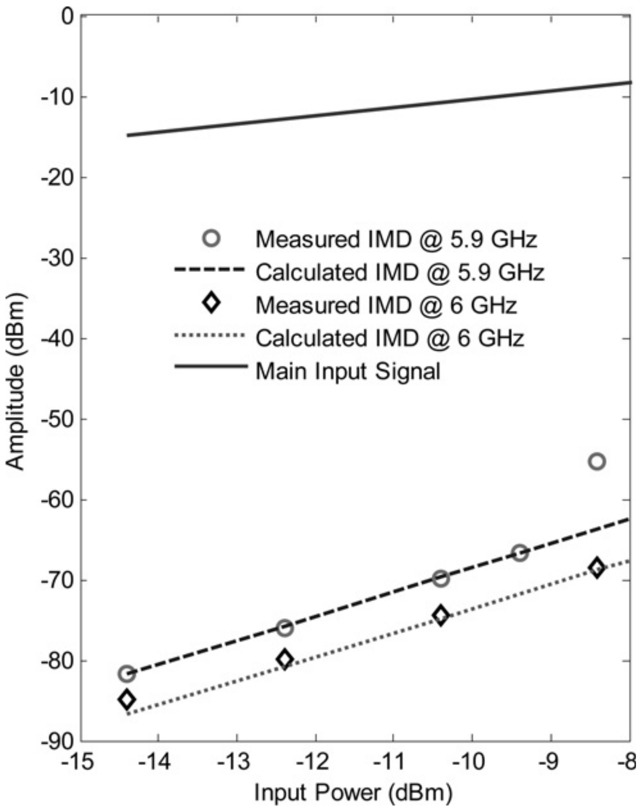

Fig. 7 *Measured IMD3 in different input power for Δf = 20 MHz at two frequencies of 5.9 and 6 GHz*

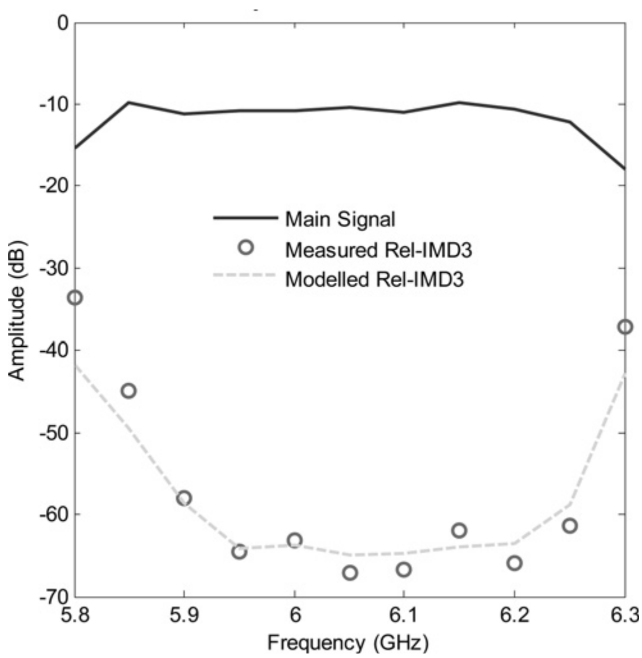

Fig. 8 *Measured and calculated IMD3 power relative to main power in two different frequencies for $P_{in} = -10$ dBm and Δf = 20 MHz*

doi: 10.1049/iet-map.2013.0528

$\Delta f = 20$ MHz and $T = 4.2$ K are shown in Fig. 7. As expected, the fundamental signal has a slope of 1 (10 dB/decade) and the IMD has a slope of 3 (30 dB/decade).

Fig. 8 shows the calculated and measured IMD power relative to the main tone at frequencies of 5.9 and 6 GHz for $P_{in} = -10$ dBm and $\Delta f = 20$ MHz. As expected the relative IMD is increased near the passband edges.

In Figs. 7 and 8, we see that the results of our proposed non-linear model have good agreement with the measured results verifying the validity of the model. Therefore by using the proposed non-linear circuit model we can produce an equivalent non-linear circuit model for every superconducting spiral resonator or filter. Then HB analysis of this non-linear circuit gives the non-linear parameters of that structure, like IMD and harmonic generation. This prediction of non-linearity helps engineers and researchers in different steps of the designing of the superconducting structures and even system designing.

5 Conclusion

In this work, a distributed non-linear circuit model for superconducting CPW rectangular-spiral resonators was presented. This model is fundamentally based on accurate non-linear circuit model for superconducting parallel coupled lines, considering simultaneously both quadratic and modulus non-linear dependencies, and gives an equivalent non-linear circuit for each spiral resonator. In the case of spiral filters which may contain a number of resonators, the proposed model can be extended to take into account the coupling between adjacent resonators. It was shown that numerical approaches based on HB method can be used for non-linear analysis of the proposed equivalent non-linear circuit. To implement the proposed model it was required to find the current distribution, which was computed by a numerical approach based on 3D-FEM.

The accuracy of the proposed model is validated by the fabrication and the measurement of a quasi-elliptic 6-pole superconducting CPW spiral filter. Non-linear measurements were performed at 4.2 K and its results show good agreement with obtaining results from our proposed non-linear model. Although the proposed model here was used for CPW resonators, it can be easily extended for superconducting spiral resonators in the form of microstrip or stripline using a similar procedure.

6 Acknowledgments

The authors thank Prof. T.M. Klapwijk for making this research possible by hosting S.M.H. Javadzadeh at the Kavli Institute of Nanoscience, Faculty of Applied Sciences, Delft University of Technology, Delft, the Netherlands.

7 References

1 Xu, D., Yip, S.K., Sauls, J.A.: 'Nonlinear Meissner effect in unconventional superconductors', *Phys. Rev. B*, 1995, **51**, (22), p. 16233
2 Dahm, T., Scalapino, D.J.: 'Theory of intermodulation in a superconducting microstrip resonator', *J. Appl. Phys.*, 1997, **81**, (4), pp. 2002–2009
3 Vendik, O.G., Vendik, I.B., Samoilova, T.B.: 'Nonlinearity of superconducting transmission line and microstrip resonator', *IEEE Trans. Microw. Theory Tech.*, 1997, **45**, (2), pp. 173–178
4 Collado, C., Mateu, J., Ferrús, R., O'Callaghan, J.M.: 'Prediction of nonlinear distortion in HTS filters for CDMA communication systems', *IEEE Trans. Appl. Supercond.*, 2003, **13**, (2), pp. 328–331
5 Collado, C., Mateu, J., Menéndez, O., O'Callaghan, J.M.: 'Nonlinear distortion in a 8-pole quasi-elliptic bandpass hts filter for CDMA system', *IEEE Trans. Appl. Supercond.*, 2005, **15**, (2), pp. 992–995
6 Oates, D.E., Anderson, A.C., Sheen, D.M., Ali, S.M.: 'Stripline resonator measurements of ZS versus HRF in yba2cu3o7 thin films', *IEEE Trans. Microw. Theory Techn.*, 1991, **39**, (9), pp. 1522–1529
7 Oates, D.E., Park, S.H., Agassi, D., Koren, G.: 'Temperature dependence of intermodulation distortion in ybco', *Supercond. Sci. Technol.*, 2004, **17**, (5), p. S290
8 Eben, A.M., Bunnell, V.A., Goodson, C.J., Pease, E.K., Lee, S.C., Remillard, S.K.: 'Even and odd order intermodulation nonlinearity from superconductive microstrip lines', *IEEE Trans. Appl. Supercond.*, 2011, **21**, (3), pp. 595–598
9 Lam, C.W., Sheen, D.M., Ali, S.M., Oates, D.E.: 'Modeling the nonlinearity of superconducting strip transmission lines', *IEEE Trans. Appl. Supercond.*, 1992, **2**, (2), pp. 58–66
10 Collado, C., Mateu, J., O'Callaghan, J.M.: 'Nonlinear simulation and characterization of devices with HTS transmission lines using harmonic balance algorithms', *IEEE Trans. Appl. Supercond.*, 2001, **11**, (1), pp. 1396–1399
11 Javadzadeh, S.M.H., Farzaneh, F., Fardmanesh, M.: 'Modeling of unusual nonlinear behaviors in superconducting microstrip transmission lines', *Phys. C, Supercond.*, 2013, **486**, pp. 37–42
12 Mateu, J., Collado, C., O'Callaghan, J.M.: 'Modeling superconducting transmission line bends and their impact on nonlinear effects', *IEEE Trans. Microw. Theory Tech.*, 2007, **55**, (5), pp. 822–828
13 Hortensius, H.L., Driessen, E.F.C., Klapwijk, T.M., Berggren, K.K., Clem, J.R.: 'Critical-current reduction in thin superconducting wires due to current crowding', *Appl. Phys. Lett.*, 2012, **100**, (18), p. 182602
14 Javadzadeh, S.M.H., Farzaneh, F., Fardmanesh, M.: 'Analytical distributed non-linear model for symmetric and asymmetric superconducting parallel-coupled microstrip lines', *IET Microw. Antennas Propag.*, 2014, **8**, (6), pp. 429–436
15 Javadzadeh, S.M.H., Farzaneh, F., Fardmanesh, M.: 'Nonlinear circuit model for discontinuity of step in width in superconducting microstrip structures and its impact on nonlinear effects', *IEEE Trans. Appl. Supercond.*, 2013, **23**, (2), p. 1301208
16 Mateu, J., Collado, C., O'Callaghan, J.M.: 'Nonlinear model of coupled superconducting lines', *IEEE Trans. Appl. Supercond.*, 2005, **15**, (2), pp. 976–979
17 Talisa, S.H., Janocko, M.A., Moskowitz, C., *et al.*: 'Low-and high-temperature superconducting microwave filters', *IEEE Trans. Microw. Theory Tech.*, 1991, **39**, (9), pp. 1448–1454
18 Zhang, G., Lancaster, M.J., Huang, F.: 'A high-temperature superconducting bandpass filter with microstrip quarter-wavelength spiral resonators', *IEEE Trans. Microw. Theory Tech.*, 2006, **54**, (2), pp. 559–563
19 Roshanmanesh, S., Javadzadeh, S.M.H.: 'Wide-band spiral filter using microstrip patches to increase external and internal coupling', *Electromagnetics*, 2012, **32**, (3), pp. 161–172
20 Zhou, J., Lancaster, M.J., Huang, F.: 'HTS coplanar meander-line resonator filters with a suppressed slot-line mode', *IEEE Trans. Appl. Supercond.*, 2004, **14**, (1), pp. 28–32
21 Ma, Z., Kawaguchi, T., Kobayashi, Y., Koizumi, D., Satoh, K., Narahashi, S.: 'A miniaturized high temperature superconducting bandpass filter using CPW quarter-wavelength spiral resonators'. IEEE MTT-S, Int. Microwave Symp. Digest, June 2006, pp. 1197–1200
22 Ghamsari, B.G., Abrahams, J., Remillard, S., Anlage, S.M.: 'High-temperature superconducting spiral resonator for metamaterial applications', *IEEE Trans. Appl. Supercond.*, 2013, **23**, (3), pp. 500304–1500304
23 Ghamsari, B.G., Abrahams, J., Remillard, S., Anlage, S.M.: 'High-temperature superconducting multi-band radio-frequency metamaterial atoms', *Appl. Phys. Lett.*, 2013, **102**, (1), p. 013503
24 Agilent Technologies Inc. Advanced Design System (ADS), V. 2011
25 Gupta, K.C., Ramesh, G., Bahl, I.J., Bhartia, P.: 'Microstrip lines and slotlines' (Artech house Dedham, Massachusetts, 1979) vol. 2
26 Paul, C.R.: 'Analysis of multiconductor transmission lines' (Wiley-IEEE Press, 2007)
27 Mollai, S., Javadzadeh, S.M.H., Shishegar, A.A., Banai, A., Farzaneh, F., Fardmanesh, M.: 'Analysis of nonlinearities in superconducting microstrip straight bends; FDTD method in comparison with nonlinear circuit modeling', *J. Supercond. Novel Magn.*, 2013, **26**, (5), pp. 1827–1830
28 Javadzadeh, S.M.H., Farzaneh, F., Fardmanesh, M.: 'Current distribution and nonlinearity of open-ends and gaps in

superconducting microstrip structures', *J. Supercond. Novel Magn.*, 2013, **26**, (5), pp. 1821–1825
29 COMSOL: Multi physics v4.0. COMSOL Inc.
30 Javadzadeh, S.M.H., Bruno, A., Farzaneh, F., Fardmanesh, M.: 'Superconducting compact coplanar waveguide filters based on quarter-wavelength spiral resonators with suppressed slot-line mode', *Electromagnetics*, 2014, **34**, (1), pp. 12–18
31 EM Users Manual: Sonnet software inc., version 13.1, 2012
32 Iosad, N.N., van der Pers, N.M., Grachev, S., *et al.*: 'Texture formation in sputter-deposited ($nb_{0.7}$, ti_{03}) n thin films', *J. Appl. Phys.*, 2002, **92**, (9), pp. 4999–5005
33 Iosad, N.N., Mijiritskii, A.V., Roddatis, V.V., *et al.*: 'Properties of $(nb_{0.35}, ti_{0.15})_x\ ni_{1-x}$ thin films deposited on silicon wafers at ambient substrate temperature', *J. Appl. Phys.*, 2000, **88**, (10), pp. 5756–5759
34 Bahl, I.J.: 'Lumped elements for RF and microwave circuits' (Artech House Publishers, 2003)

doi: 10.1049/iet-map.2013.0528